ADVANCED FUNCTIONAL MATERIALS
www.afm-journal.de

Anodized ITO Thin-Film Transistors

*Yang Shao, Xiang Xiao, Longyan Wang, Yang Liu, and Shengdong Zhang**

This paper reports that the electrical, optical, and structural properties of ITO film can be significantly modulated by an anodization treatment. An ITO TFT technology based on the anodization approach is then proposed and demonstrated, which results in an ideal homo-junction device structure with the source/drain/pixel electrodes and channel region made of one single ITO layer. A preliminary device fabrication at room temperature shows the resulting TFT has an on/off current ratio exceeding 1×10^8, a saturation mobility of 29.0 $cm^2 V^{-1} s^{-1}$, and a subthreshold swing of 0.20 V per decade. This technology also allows a feasible V_T adjustment and muti-V_T implementation.

1. Introduction

Oxide semiconductor (OS) thin-film transistors (TFTs) are expected to replace conventional Si based TFTs due to their attractive properties such as high carrier mobility, steep subthreshold swing, good electrical stability, high optical transparency and favorable processing versatility.[1–4] Numerous OS materials have been investigated for fabricating the OS TFTs, and the carrier mobility of ≈100 $cm^2 V^{-1} s^{-1}$ with the OS TFTs has been realized,[5–10] demonstrating the significant potential of the OS materials for TFT applications.

Among those OS materials, indium tin oxide (ITO) has been extensively used as the transparent conductive film material and become the indispensable part of modern display devices by virtue of its relatively low resistivity (≈10^{-4} Ω cm) and high visible transmittance (>85%).[11,12] Now that ITO is indispensable, it should be a good conception to establish an "All by ITO" technology in which the source/drain electrodes, channel layers and even the gate electrodes of TFTs, together with the pixel electrodes of display devices are all made of the ITO material. It is obvious that the "All by ITO" technology enables a much simplified and cost effective fabrication process for display devices, and also leads to the realization of a new fully transparent electronic device technology.[13] However, the "All by ITO" technology is difficult to realize at present despite of the attractive advantages. The inherent high carrier density and polycrystalline nature with the ITO are two major obstacles to using it as the active layers of TFTs although it is an oxide semiconductor in itself and could be used as the active layers of TFTs. The high carrier density would prevent the devices from being switched-off normally; and the polycrystalline nature would bring about the poor device performance uniformity over large area.

In an earlier effort to fabricate ITO TFTs, the sputtered ITO nano-clusters diffracting into the masked shadow regions were used to form an ultra-thin channel layer.[14] Clearly, this technique has a difficulty in controlling the morphology of the self-assembled film and is not compatible with the mainstream flat panel display (FPD) technologies. An alternative effort to build the ITO TFTs was to make the TFTs have a junctionless structure.[15] In doing so, for turning the TFT off properly, the channel layer must be thin enough and the gate capacitance must be large enough to enable the channel layer depleted fully.

Therefore, the feasible technology for ITO TFTs with a combination of simple process and high device performance has not been well established so far. On the other hand, a homo-junction (HJ) structure with source/drain and channel layers made of the same material is a preferable structure for TFTs. In the case of poly-Si TFTs, this kind of structure can be easily obtained by a self-aligned ion implantation to dope the source/drain regions. However, it is difficult to adopt this structure in the case of OS TFTs. In this work, an "All by ITO" TFT technology featuring the ideal homo-junction device structure is realized by introducing an anodic oxidation (anodization) technique to locally tailor the ITO properties for the first time.

The anodic oxidation technique has often been used to grow the metal oxide dielectrics due to the favorable features such as simple equipment requirement, low cost and high throughput.[16–18] The formation of anodic oxide films has been a long discussion since 1934.[19] Although numerous models have been proposed to explain the kinetic, thermodynamic, structural and electronic properties, no single theory has yet emerged to provide comprehensive descriptions of the individual processes and explanations for the differences because of the complexity of various real metal–oxide systems. In spite of this, it is commonly recognized that a large number of metals when anodically polarized, exhibit the so-called high-field conduction behavior which suggests a thermally activated, field supporting hopping transport during the oxide growth.[20,21] Furthermore, the oxide film growth is largely or exclusively resulted from the high-field assisted inward movement of oxygen ions from the film/solution interface to the metal/film interface.[21]

On the other hand, ITO is usually a highly degenerate n-type OS so that it acts more like a metal than a semiconductor. It

Y. Shao, X. Xiao, L. Wang, Y. Liu, Prof. S. Zhang
School of Electronic and Computer Engineering
Peking University
Shenzhen 518055, China
E-mail: zhangsd@pku.edu.cn

DOI: 10.1002/adfm.201400263

can thus be reasonably assumed that when a treatment like the anodic oxidation is applied to ITO film, the high-field-assisted inward migration of oxygen ions should also take place, having the inside oxygen vacancy concentration, in other words the carrier concentration reduced. Furthermore, since the motion of oxygen ions is assisted by the electric field, the reduced amount in the oxygen vacancies should be dependent on the anodic oxidation potential, similar to the case in the anodic oxidation of metals.[22] This potentially allows the anodic oxidation treatment a promising way of flexibly modulating the electrical property of ITO films.

In this work, we explored the anodic oxidation treatment process of ITO films to realize the "All by ITO" TFT technology for the first time. To demonstrate the feasibility of this technique, the resulting evolution of the electrical and optical properties as well as the crystal structure with the ITO film from the anodic oxidation treatment was investigated. TFTs with the anodized ITO as the channel layers were also fabricated. All the fabrication steps were performed at room temperature, making the approach appealing to low temperature transparent flexible electronics. Another key finding of this work is the utility of a tunable threshold voltage (V_T) technology by means of the anodic oxidation process.

2. Results and Discussion

The anodization induced electrical property modulation in the ITO film was studied first. The initial ITO film of 100 nm was deposited by RF sputtering at room temperature. The proposed anodization process was then performed with the deposited ITO film with the details given in the Experimental Section. **Figure 1** shows the ITO sheet resistance (resistivity) versus V_a, the anodic oxidation (anodization) voltage. V_a is defined as the voltage value at which the anodization process is switched from a constant current mode to a constant voltage one as described in the Experimental Section. The inset in Figure 1 is the schematic anodic oxidation equipment. It is seen that the ITO sheet resistance (resistivity) increases significantly with increasing the V_a value and there is an increase of more than eight orders of magnitude in the resistivity for V_a higher than 20 V. This verifies the effectiveness of the proposed anodic oxidation treatment. For the ITO film deposited at room temperature, the carriers are primarily released from oxygen vacancies rather than the Sn dopants which are not efficiently activated.[23–25] It is thus deduced that the significant increase of the ITO resistivity results from the significant reduction of the inner oxygen vacancy concentration. When the anodic oxidation is performed, an electric field is established across the ITO film, and the current flowing through the ITO film is mainly in the form of ionic conduction from the oxygen ions migrating from the electrolyte into the ITO film under the drive of the electric field. The oxygen vacancies in the ITO film are thus gradually occupied by the injected oxygen ions, so that the concentration of carriers in the ITO film is decreased, that is, the resistivity of the ITO is increased. For the higher V_a, the constant current period of the anodization process is accordingly longer. This means that more oxygen ions are driven into the ITO film, leading to the lower oxygen vacancy concentration, namely the higher resistivity of the ITO film. Thus, the ITO resistivity increases significantly with increasing the V_a value as shown in Figure 1. When V_a is high enough, the number of the driven-in oxygen ions is so big that the oxygen vacancies in the ITO film are mostly occupied. As a result, the increase in the resistivity of the ITO with further increasing V_a gets less significant as shown in Figure 1.

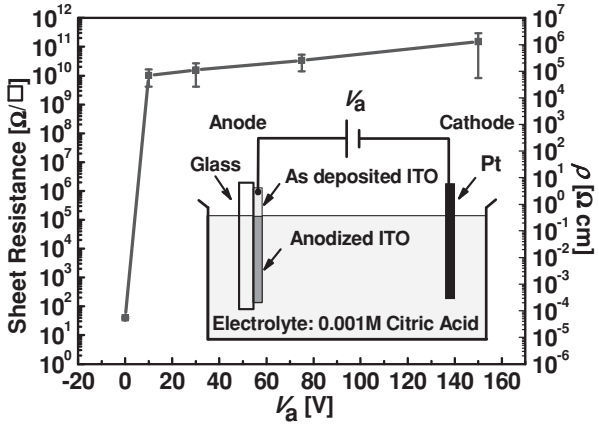

Figure 1. Sheet resistance (left axis) and resistivity (right axis) of the ITO film as a function of the anodization voltage V_a. The ITO film was 100 nm thick and deposited by RF magnetron sputtering on the glass substrates. The inset is the schematic diagram of the anodic oxidation equipment where the ITO film exposed to the electrolyte is anodized.

The potential of the anodic oxidation approach in fabricating TFTs was then investigated. The fabricated TFT is in the bottom-gate architecture as shown in **Figure 2**a. The Ta_2O_5 gate dielectric and the ITO active film are 200 and 100 nm thick, respectively. Although the gate electrode was not patterned for simplification sake, it serves the purpose of investigating the fundamental properties of the devices. Details of the fabrication process can be found in the Experimental Section. The unique step in the fabrication is the patterned anodization as shown in Figure 2a, where the targeted source/drain regions are covered with the photoresist (PR) layer, keeping the underneath ITO free of the anodization; and the channel region is exposed to the electrolyte to be anodized. As a result, the covered ITO for the source/drain regions remains high conductive and the exposed ITO for the channel region is modulated in the electrical property to meet the threshold voltage requirements. It should be noted that the resulting device is intrinsically in the ideal HJ structure. Figure 2b displays the typical transfer characteristics of the anodized HJ ITO TFTs at V_a of 50 V. The channel width and length of the TFTs are both 100 μm. The ITO TFTs exhibited a V_T of 1.05 ± 0.28 V, subthreshold swing (SS) of 0.20 V/decade, saturation mobility (μ_{sat}) of 29.0 ± 1.2 $cm^2 V^{-1} s^{-1}$, and on/off current ratio of >1 × 10^8. The μ_{sat} and V_T values were derived from a linear fitting to the $I_{DS}^{1/2}$ versus V_{GS} plot (I_{DS} is the drain-to-source current and V_{GS} is the gate-to-source voltage). The data shown here is the average value of the electrical performances over twenty ITO TFTs fabricated in one run. A turn-on voltage (V_{ON}), which is defined as the gate voltage corresponding to the onset of I_{DS} increase, is nearly 0 V. The proper V_{ON} with a small SS is favorable for low power consumption applications. The output characteristics of the ITO

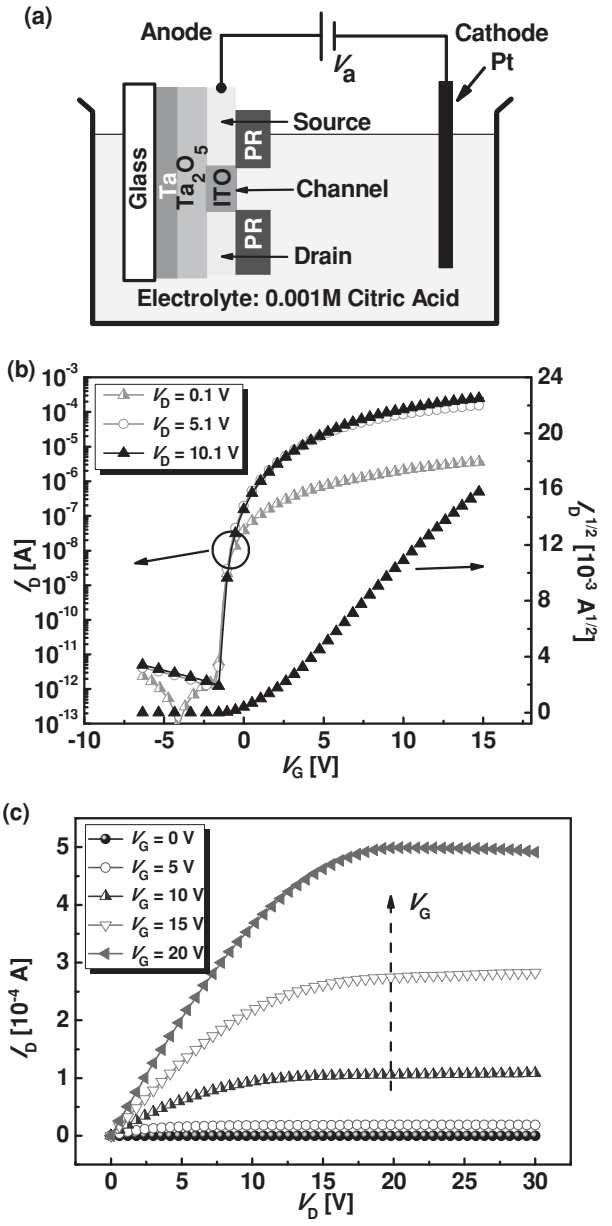

Figure 2. a) Schematic cross-sectional view of the homo-junction ITO TFT fabrication in the anodization process. The source/drain and channel regions were defined by a patterned anodization step. The ITO sections covered with the PR were for the source/drain regions which remained high conductive after the anodization step. The ITO section exposed to the electrolyte was for the channel region which was anodized during the anodization period. b,c) Representative transfer and output characteristics of the anodized ITO TFTs at V_a = 50 V, respectively.

TFT shown in Figure 2c demonstrate a typical n-channel transistor behavior. Linear behaviors of I_{DS} at low V_{DS} indicate that a good Ohmic contact between the channel layer and source/drain electrodes was realized. Additionally, the output characteristics exhibit a clear pinch-off and drain current saturation. It is thus verified that high performance of TFTs can be obtained using the anodization technique. It has also been reported that the density of oxygen vacancies in the anodic oxide layer decreases gradually from the metal/oxide interface to the

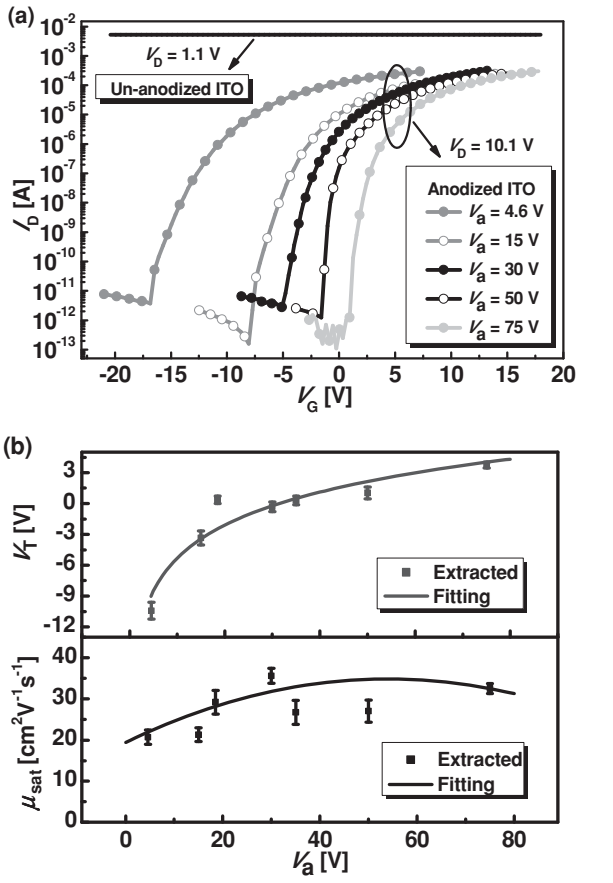

Figure 3. a) Transfer characteristics of the un-anodized and the anodized ITO TFTs at the different anodization voltages V_a. The un-anodized one did not show a normal transistor behavior due to the too conductive channel. b) Extracted V_T and μ_{sat} values from the anodized ITO TFTs versus the corresponding anodization voltages V_a. Each plotted point represents the average value of forty devices with the standard deviation plotted as error bars. Fitting lines are plotted alongside data symbols.

oxide/electrolyte interface.[22,26] Therefore, it can be reasonably deduced that the carrier concentration in the anodized ITO film gradually increases from the top surface to the inside. This spatially non-uniform distribution of oxygen vacancy (carrier) concentration in the active layer is helpful for enhancing the TFT performance because the high carrier concentration adjacent to the gate insulator is for the high mobility and the low carrier concentration close to the top surface is for the suitable V_T.[8,27]

We have also explored the potential of using the anodization treatment to modulate the threshold voltage of ITO TFTs. As shown in **Figure 3**a, no current switching behavior was observed if the active layer is just the as-deposited ITO film without the anodization step. It is obviously because the as-deposited ITO film is too conductive to be depleted. In contrast, all the anodized ITO TFTs show the reasonable transistor behaviors. Furthermore, V_T of the TFTs can be adjusted in a wide range from –10.4 ± 0.8 V to 3.7 ± 0.3 V with V_a changing from 4.6 V to 75 V, allowing the device operation to switch from a depletion mode to an enhancement mode. In this way, by simply changing the V_a value during the anodic oxidation, it is feasible to: i) shift V_{ON} close to 0 V; ii) set, a priori, the device operation

either to enhancement or to depletion mode; and iii) allow a separate TFT V_T control on the same substrate via a separate anodic oxidation step with different V_a, namely, a multiple-V_T technology. The extracted V_T and μ_{sat} values of the TFT versus V_a are presented in Figure 3b. There is a clear monotonic relationship between V_T and V_a. The monotonic increase of V_T with increasing V_a is attributed to the monotonic reduction of the carrier concentration in the ITO channel region as shown in Figure 1. While V_T varies considerably with V_a, the saturation mobility μ_{sat} exhibits less sensitive to V_a, initially having a slight increase and then a slight decrease with the V_a increase. The initial increase in μ_{sat} with the V_a increase is likely due to the decrease in the concentration of the oxygen vacancies, which act as donor defects and contribute to increasing the density of charged scattering centers. The slight decrease in μ_{sat} at the higher V_a can be attributed to an over-increased oxygen content that surpasses the critical value at which a stoichiometric ITO film is formed. The excess oxygen atoms in interstitial positions introduce the interstitial defects and neutral scattering defects, resulting in the degradation of the mobility. Another plausible explanation is based on the percolation conduction model where the saturation mobility usually slightly decreases with the decrease of carrier concentration due to the increased potential barrier.[28]

Moreover, thanks to the high transparent conductive ITO film, a self-aligned bottom-gate homo-junction TFT technology based on the proposed anodization technique was also realized successfully. **Figure 4**a shows the photograph of a process-finished wafer on the left side with the Peking University Logo underneath and the top view photograph of a finished TFT on the right side. The schematic cross-sectional view of the key self-aligned fabrication step is shown in the inset of Figure 4b, where, the ITO layer allows the negative photoresist on it to be exposed to UV light from the glass backside, and the metal gate electrode blocks the path of the UV light to the photoresist on the channel region which can be removed in the subsequent developing step. The detailed fabrication process for the self-aligned ITO TFT is shown in Figure S1 (Supporting Information). The self-aligned technology minimizes the overlap capacitance between the gate and source/drain and number of masks needed, being favorable for high speed circuit applications.

The representative transfer and output characteristics of the self-aligned devices are shown in Figure 4b and 4c, respectively. While the device performance is a little worse than the above one due to the non-optimized process, it is still excellent with an on/off current ratio exceeding 1×10^8, a saturation mobility of 20.9 $cm^2\ V^{-1}\ s^{-1}$, and subthreshold swing of 0.77 V per decade. Figure 4d shows the extracted V_T values versus the anodization voltages V_a for the fabricated self-aligned ITO TFT. The V_T vlues increase monotonically from -16.8 ± 1.5 V to -2.8 ± 1.1 V with V_a changing from 10 V to 100 V, showing a wide tunable range. The self-aligned device results further manifest the advantages of the proposed anodization technique in making high performance TFTs at low cost.

Figure 5 shows the optical transmittances of the as-deposited ITO film and the anodized one at $V_a = 30$ V. As is evident from this result, the average transmittance at the visible-light wavelengths (400–700 nm) is increased from 81% to 89%. This increase can be attributed to the decrease of the number of oxygen vacancies in the anodized film. It is believed that the as-deposited ITO film is less stoichiometric or more metallic in structure, resulting thereby in the compounds with lower

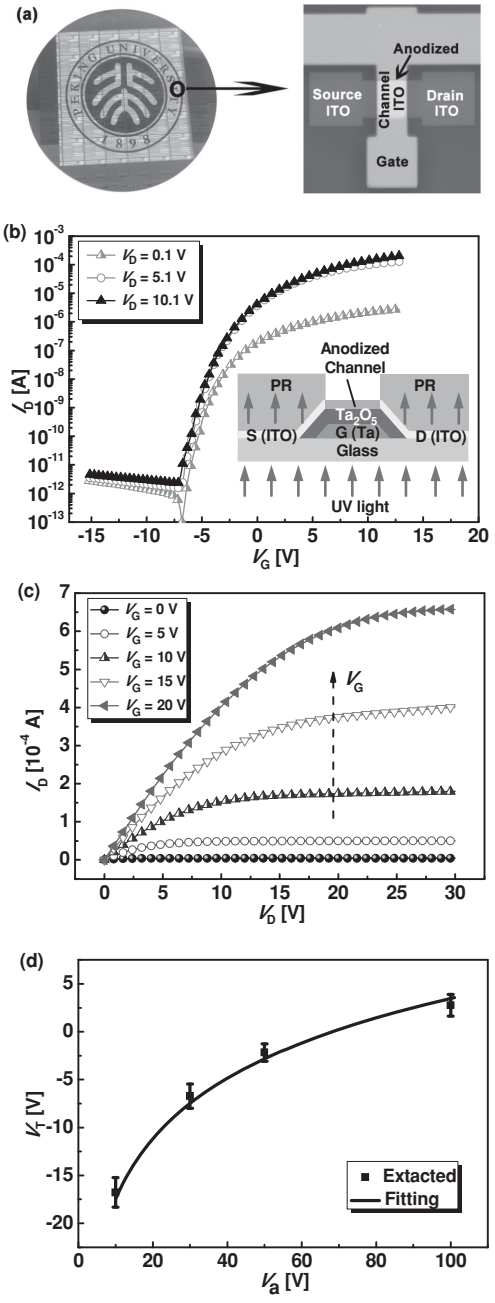

Figure 4. Schematic fabrication and representative characteristics of the self-aligned anodized ITO TFTs. a) Photograph of a process-finished wafer on the left side with the Peking University Logo underneath and that of a finished TFT top view on the right side; b) transfer characteristics of the anodized ITO TFT at $V_a = 50$ V. The inset is the schematic cross-sectional view of the key fabrication step for the self-aligned homo-junction ITO TFT; c) output characteristics of the anodized ITO TFT at $V_a = 50$ V and d) extracted V_T values from the self-aligned TFTs versus the anodization voltages V_a. Each plotted point represents the average value of forty devices with the standard deviation plotted as error bars. Fitting line is plotted alongside data symbols.

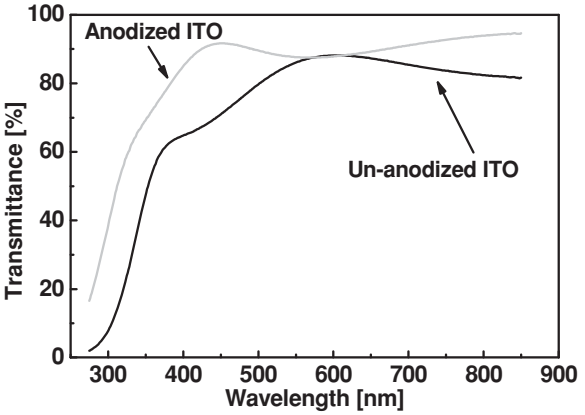

Figure 5. Optical transmission spectra of the ITO films (≈100 nm) without and with the anodic oxidation treatment at the anodization voltage V_a of 30 V.

valence state and poor optical transmittance.[29–32] The anodic oxidation treatment helps restore the stoichiometry of the ITO film and thus improve the transparency.

In addition, the microstructure of ITO films was investigated using X-ray diffraction (XRD) to have an insight into the effects of the proposed anodization technique on crystal structure of ITO films. It is known that the ITO films deposited at low temperature are usually in amorphous phase and can be transferred to the poly-crystalline phase with annealing at a high temperature. In this work, both the as-deposited and anodized ITO films were annealed in nitrogen atmospheres at the temperature ranging from 150 °C to 300 °C. **Figure 6** displays the XRD patterns of the resulting ITO films with and without the anodic oxidation treatment. It is observed that while the as-deposited ITO film was recrystallized at the annealing temperature of 300 °C, the anodized one remains amorphous. This implies that the anodization raises the temperature at which the ITO film begins to recrystallize. This observation here is quite different from what have been disclosed in the earlier studies[33,34] where the ITO film deposited with more oxygen introduction

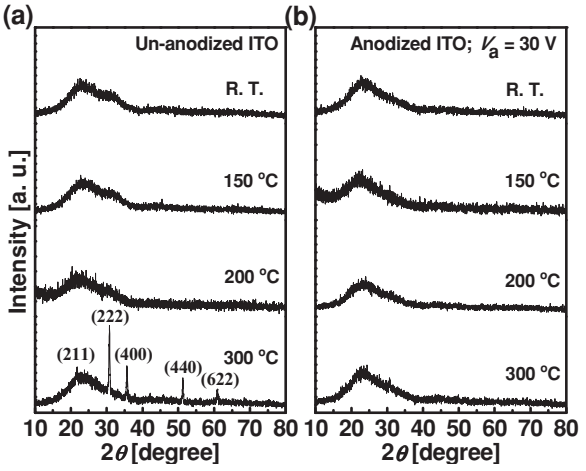

Figure 6. X-ray diffraction patterns of the ITO films (≈100 nm) grown on glass substrates at room temperature and annealed at the relatively high temperature with a) un-anodized and b) anodized at V_a of 30 V.

into the sputtering atmosphere showed a lower recrystallization temperature. It is known that the ITO films with more oxygen vacancies tend to grow along the crystallographic plane[33,35–37] that requires a higher atomic mobility and thereby a higher temperature to promote the recrystallization.[38] However, the anodized ITO film shown a higher recrystallization temperature than the un-anodized one although it has a much lower oxygen vacancy concentration. The rise of the recrystallization temperature is likely due to the migration and incorporation into the ITO films of the oxygen ions, hydroxide ions and other anions from the electrolyte during the anodization process.[21,39] The migration and incorporation of those anions may change the microstructure of the ITO films to some extent, and/or disturb the crystal growth, leading to the increased recrystallization temperature. Anyway, the anodization induced rise of the recrystallization temperature is a desired property since the amorphous active films are always preferable for large area electronics applications.

At last, it is worth mentioning that the proposed anodization technique can also be applied to other transparent conductive metal oxide films such as SnO_2, ZnO, as well as IGZO. Even more, it can also be applied to some metal films such as In, Zn and Sn to form novel TFT structures, like source of metal, channel of metal oxide and drain of metal. Therefore, the proposed technique may enable a new TFT technology with high device performance, low processing temperature and low fabricating cost.

3. Conclusion

We have demonstrated that the anodization process can flexibly and significantly modulate the electrical, optical and structural characteristics of the ITO films. Homo-junction TFTs with source/drain and channel layers all made of the same ITO layer were implemented at room temperature in the proposed process. Despite the preliminary fabrication, the resulting TFTs showed an on/off current ratio exceeding 1×10^8, a saturation mobility of 29.0 $cm^2\ V^{-1}\ s^{-1}$ and a subthreshold swing of 0.20 V per decade. Also, the proposed technique enables a self-aligned homo-junction and a multi-V_T TFT technology. In addition, the proposed technique can improve the optical transmittance and suppress the phase transition of the ITO film from amorphous to crystalline structure. With all these favorable features, the proposed technique enables a new TFT technology with high device performance, low processing temperature and low fabricating cost, which is well suitable for flexible large area electronics applications.

4. Experimental Section

Anodic Oxidation of ITO: The anodization process was conducted in a 0.001 M citric acid solution with a platinum foil as a counter electrode (cathode) as shown in the inset of Figure 1. It was initially in a constant current mode (CC mode) and then a constant voltage mode (CV mode). In the CC period, the current density flowing though the ITO area immersed in the solution was maintained at 0.2 mA cm^{-2} and the anode voltage accordingly kept going up with the increase of the ITO resistivity. Once the anode voltage rose to one target value, the anodization

process was then switched to CV period when the anode voltage was fixed at the target value and the current accordingly gradually decayed. Here, the target anode voltage is defined as the anodization voltage V_a which was varied in the range of 5–100 V in this experiment.

Homo-Junction ITO TFT Fabrication: The process began with a sputtered deposition of the 200 nm Ta film as the gate electrode and an anodic formation of the 200 nm Ta_2O_5 gate dielectric from the Ta film. A 100 nm ITO film was then deposited by RF magnetron sputtering at room temperature using an ITO target (90 wt% In_2O_3 and 10 wt% SnO_2) with the power of 80 W, working pressure of 1 Pa, and pure Ar (40 sccm) gas atmosphere. A conventional photolithography was then performed to form the PR patterns as shown in Figure 2a. Finally, the patterned anodization step related above was performed to form the source/drain and channel regions.

Self-Aligned Homo-Junction Transistor Fabrication: The Ta film of 200 nm was first patterned to form the gate electrode before the anodic formation of the Ta_2O_5 gate dielectric of 200 nm. Then, the ITO film of 100 nm was deposited using the same growth condition at room temperature as mentioned above. After the negative PR coating, the UV light exposure was performed from the wafer backside, so that the Ta gate electrode blocked the path of the UV light to the PR on the channel region which was subsequently removed in the developing step. In this way, the self-aligned channel region was defined and formed after the anodization step was done as shown in the inset of Figure 4b.

Supporting Information

Supporting Information is available from the Wiley Online Library or from the author.

Acknowledgements

This work was conducted in Shenzhen TFT and advanced Display Lab and supported by National Natural Science Foundation of China (NSFC) under project 61274084 and Shenzhen scientific program (JCYJ20120829170028552). The authors also thank L. Zhang and X. Zhou for helpful discussions.

Received: January 24, 2014
Revised: February 13, 2014
Published online: March 28, 2014

[1] K. Nomura, H. Ohta, A. Takagi, T. Kamiya, M. Hirano, H. Hosono, *Nature* **2004**, *432*, 488.
[2] E. Fortunato, P. Barquinha, R. Martins, *Adv. Mater.* **2012**, *24*, 2945.
[3] R. A. Street, *Adv. Mater.* **2009**, *21*, 2007.
[4] T. Kamiya, K. Nomura, H. Hosono, *J. Display Technol.* **2009**, *5*, 273.
[5] J. Jang, R. Kitsomboonloha, S. L. Swisher, E. S. Park, H. Kang, V. Subramanian, *Adv. Mater.* **2013**, *25*, 1042.
[6] H.-W. Zan, C.-C. Yeh, H.-F. Meng, C.-C. Tsai, L.-H. Chen, *Adv. Mater.* **2012**, *24*, 3509.
[7] L. Wang, M.-H. Yoon, A. Facchetti, T. J. Marks, *Adv. Mater.* **2007**, *19*, 3252.
[8] S. I. Kim, C. J. Kim, J. C. Park, I. Song, S. W. Kim, H. Yin, E. Lee, J. C. Lee, Y. Park, *IEDM Tech. Dig.* **2008**, 73.
[9] L. Wang, M.-H. Yoon, G. Lu, Y. Yang, A. Facchetti, T. J. Marks, *Nat. Mater.* **2006**, *5*, 893.
[10] E. Fortunato, P. Barquinha, A. Pimentel, L. Pereira, G. Gonçalves, R. Martins, *Phys. Status Solidi (RRL)* **2007**, *1*, R34.
[11] R. B. H. Tahar, T. Ban, Y. Ohya, Y. Takahashi, *J. Appl. Phys.* **1998**, *83*, 2631.
[12] H. Kim, C. M. Gilmore, A. Piqué, J. S. Horwitz, H. Mattoussi, H. Murata, Z. H. Kafafi, D. B. Chrisey, *J. Appl. Phys.* **1999**, *86*, 6451.
[13] S. Y. Park, K. H. Ji, H. Y. Jung, J.-I. Kim, R. Choi, K. S. Son, M. K. Ryu, S. Lee, J. K. Jeong, *Appl. Phys. Lett.* **2012**, *100*, 162108.
[14] A. Lu, J. Sun, J. Jiang, Q. Wan, *IEEE Electron Device Lett.* **2010**, *31*, 1137.
[15] J. Jiang, J. Sun, W. Dou, Q. Wan, *IEEE Electron Device Lett.* **2012**, *33*, 65.
[16] L. A. Majewski, R. Schroeder, M. Grell, *Adv. Mater.* **2005**, *17*, 192.
[17] M. Mizukami, N. Hirohata, T. Iseki, K. Ohtawara, T. Tada, S. Yagyu, T. Abe, T. Suzuki, Y. Fujisaki, Y. Inoue, S. Tokito, T. Kurita, *IEEE Electron Device Lett.* **2006**, *27*, 249.
[18] L. Lan, J. Peng, *IEEE Trans. Electron Devices* **2011**, *58*, 1452.
[19] A. Güntherschulze, H. Betz, *Z. Phys.* **1934**, *92*, 367.
[20] M. J. Dignam, in *Comprehensive Treatise of Electrochemistry*, Vol. *4* (Eds: J. O'M. Bockris, B. E. Conway, E. Yeager, R. E. White), Plenum Press, New York **1981**, Ch. 5.
[21] M. M. Lohrengel, *Mater. Sci. Eng.* **1993**, *11*, 243.
[22] E. Sikora, J. Sikora, D. D. Macdonald, *Electrochim. Acta* **1996**, *41*, 783.
[23] Y. Shigesato, D. C. Paine, *Appl. Phys. Lett.* **1993**, *62*, 1268.
[24] H. Morikawa, M. Fujita, *Thin Solid Films* **2000**, *359*, 61.
[25] S. B. Lee, J. C. Pincenti, A. Cocco, D. L. Naylor, *J. Vac. Sci. Technol. A* **1993**, *11*, 2742.
[26] T. Hurlen, C. Simon, W. Wilhelmsen, S. Hornkjøl, E. Gulbrandsen, *Electrochim. Acta* **1989**, *34*, 519.
[27] M. A. Marrs, C. D. Moyer, E. J. Bawolek, R. J. Cordova, J. Trujillo, G. B. Raupp, B. D. Vogt, *IEEE Trans. Electron Devices* **2011**, *58*, 3428.
[28] T. Kamiya, K. Nomura, H. Hosono, *Appl. Phys. Lett.* **2010**, *96*, 122103.
[29] J. C. C. Fan, J. B. Goodenough, *J. Appl. Phys.* **1977**, *48*, 3524.
[30] W. G. Haines, R. H. Bube, *J. Appl. Phys.* **1978**, *49*, 304.
[31] K. Carl, H. Schmitt, I. Friedrich, *Thin Solid Films* **1997**, *295*, 151.
[32] Z. Ovadyahu, B. Ovryn, H. W. Kraner, *J. Electrochem. Soc.* **1983**, *130*, 917.
[33] C. Guillén, J. Herrero, *J. Appl. Phys.* **2007**, *101*, 073514.
[34] M. Buchanan, J. B. Webb, D. F. Williams, *Appl. Phys. Lett.* **1980**, *37*, 213.
[35] P. Thilakan, C. Minarini, S. Loreti, E. Terzini, *Thin Solid Films* **2001**, *388*, 34.
[36] S.-I. Jun, T. E. McKnight, M. L. Simpson, P. D. Rack, *Thin Solid Films* **2005**, *476*, 59.
[37] C. G. Choi, K. No, W.-J. Lee, H.-G. Kim, S. O. Jung, W. J. Lee, W. S. Kim, S. J. Kim, C. Yoon, *Thin Solid Films* **1995**, *258*, 274.
[38] A. E. Hichou, A. Kachouane, J. L. Bubendorff, M. Addou, J. Ebothe, M. Troyon, A. Bougrine, *Thin Solid Films* **2004**, *458*, 263.
[39] A. J. Brock, G. C. Wood, *Electrochim. Acta* **1967**, *12*, 395.